LANGMUIR Article
Cite This: Langmuir 2017, 33, 11246-11256 pubs.acs.org/Langmuir

The Composition of the Mobile Phase Affects the Dynamic Chiral Recognition of Drug Molecules by the Chiral Stationary Phase

Binwu Zhao,[†] Priyanka A. Oroskar,[†] Xiaoyu Wang,[‡] David House,[†] Anil Oroskar,[†] Asha Oroskar,[†] Cynthia Jameson,[§] and Sohail Murad*[,‡]

[†]Orochem Technologies, Inc., 340 Shuman Boulevard, Naperville, Illinois 60563, United States

[‡]Department of Chemical Engineering, Illinois Institute of Technology, 10 West 33rd Street, Perlstein Hall, Chicago, Illinois 60616, United States

[§]Department of Chemical Engineering, University of Illinois at Chicago, 810 South Clinton Street, Chicago, Illinois 60607, United States

ABSTRACT: More than half of all pharmaceuticals are chiral compounds. Although the enantiomers of chiral compounds have the same chemical structure, they can exhibit marked differences in physiological activity; therefore, it is important to remove the undesirable enantiomer. Chromatographic separation of chiral enantiomers is one of the best available methods to get enantio-pure substances, but the optimization of the experimental conditions can be very time-consuming. One of the most widely used chiral stationary phases, amylose tris(3,5-dimethylphenyl carbamate) (ADMPC), has been extensively investigated using both experimental and computational methods; however, the dynamic nature of the interaction between enantiomers and ADMPC, as well as the solvent effects on the ADMPC-enantiomer interaction, are currently absent from models of the chiral recognition mechanism. Here we use QM/MM and molecular dynamics (MD) simulations to model the enantiomers of flavanone on ADMPC in either methanol or heptane/2-propanol (IPA) (90/10) to elucidate the chiral recognition mechanism from a new dynamic perspective. In atomistic MD simulations, the 12-mer model of ADMPC is found to hold the 4/3 left-handed helical structure in both methanol and heptane/IPA (90/10); however, the ADMPC polymer is found to have a more extended average structure in heptane/IPA (90/10) than in methanol. This results from the differences in the distribution of solvent molecules close to the backbone of ADMPC leads to changes in the distribution of the (φ, ψ) dihedral angles of the glycoside bond (between adjacent monomers) that define the structure of the polymer. Our simulations have shown that the lifetime of hydrogen bonds formed between ADMPC and flavanone enantiomers in the MD simulations are able to reproduce the elution order observed in experiments for both the methanol and the heptane/IPA solvent systems. Furthermore, the ratios of hydrogen-bonding-lifetime-related properties also capture the solvent effects, in that heptane/IPA (90/10) is found to make the separation between the two enantiomers of flavanone less effective than methanol, which agrees with the experimental separation factors of 0.9 versus 0.4 for R/S, respectively.

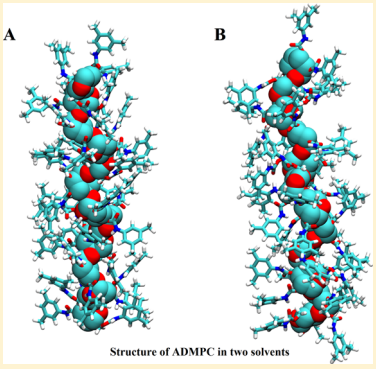

Structure of ADMPC in two solvents

INTRODUCTION

Many drug molecules have one or more chiral centers, and often these are key to their physiological functions.[1] A molecule with a single chiral center has two enantiomers, often referred to as either S or R enantiomers, which have the same molecular composition but different three-dimensional structures.[2] The structures of enantiomers are the mirror images of each other, but are not superimposable. Enantiomers of drugs could have very different pharmacological activities in living systems since the human body is a highly chiral environment.[3] The effects of different enantiomers are often markedly different as a consequence of their differential interaction with chiral targets such as receptors, enzymes, and ion channels. One enantiomer could have a beneficial therapeutic value; the other could either be inactive, have a distinctly different activity, or even have an undesirable activity.[4] One well-known example of the different effects that each enantiomer might have is thalidomide,[5,6] which was used to control nausea as well as to alleviate morning sickness in pregnant women but later was found to cause approximately 10 000 children to be born with deformed limbs, brain defects, or other developmental deformities. Later, it was shown that the S enantiomer is more teratogenic than the R enantiomer. Since the revelation of these effects of thalidomide, the issue of drug chirality has become a major theme in the design and development of new drugs. Most pharmaceutical companies only manufacture enantio-pure drugs, either by de novo development of an enantiomerically pure drug or by switching from an existing racemic drug to its isomers in pure

Special Issue: Tribute to Keith Gubbins, Pioneer in the Theory of Liquids

Received: July 5, 2017
Revised: August 14, 2017
Published: August 21, 2017

DOI: 10.1021/acs.langmuir.7b02337
Langmuir 2017, 33, 11246−11256

form. The design of such a purification system for separation of racemates to create an enantio-pure product is challenging.

One of the most effective methods of separating chiral molecules is chromatography, such as gas chromatography (GC)[7,8] and high performance liquid chromatography (HPLC).[9,10] Other methods include capillary electrophoresis (CE)[11,12] and chiral crystallization.[13,14] Chromatography is a method that separates mixtures. The mixture is first dissolved in a solvent, preferably the mobile phase. The mobile phase carries the mixture through a column filled with the stationary phase.[15] Different components in the mixture have different interactions with the stationary phase, which causes them to travel at different rates through the column, thus causing them to separate. The chromatographic process of separation is intrinsically a dynamic process. Chiral stationary phases (CSPs) are specially made for chromatographic separation of chiral substances. Many different types of CSPs have been synthesized and commercialized, such as Pirkle or brush types,[16−18] polysaccharide-based,[19−21] cavity,[22,23] ligand exchange,[24,25] and so forth. Of all the CSPs available on the market, polysaccharide-based CSPs, especially derivatives of cellulose and amylose, are the most widely used, because of their efficiency, versatility, and durability.[26−28]

The optimization of a chiral chromatography process needs to take many factors into consideration: the choice of CSPs,[29] mobile phases and any modifiers,[30] column temperature,[31,32] and the pH conditions.[33] The usual empirical approaches to examine the various combinations is tedious and time-consuming. For example, there are many options even for just the polysaccharide-based CSPs, which can be categorized based on their derivatization and whether they are coated or covalently bound to the modified silica gel support. Figure 1 shows two examples of derivatives of amylose that are commonly used. The selection of mobile phases is critical, in that the enantiomers should be soluble in the mobile phase, but the chiral phase hydrogen-bonded to the support must be insoluble, else the latter will come off the silica gel support. The mobile phase should facilitate the interactions between the CSPs and enantiomers, yet be nonreactive with them. A number of suitable mobile phases have been used including aliphatic hydrocarbon-alcohol blends such as heptane and 2-propanol (IPA), polar phases such as alcohols (methanol, ethanol, etc.), alcohol blends, acetonitrile, alcohol−water blends, and water. Sometimes modifiers may need to be added to the mobile phase to reduce secondary interactions, which cause the dispersion (peak broadening) of the analyte.[34] Therefore, to separate a particular pair of enantiomers, there could be eight CSPs, five mobile phases, and three modifiers, or 120 combinations that must be tested experimentally.

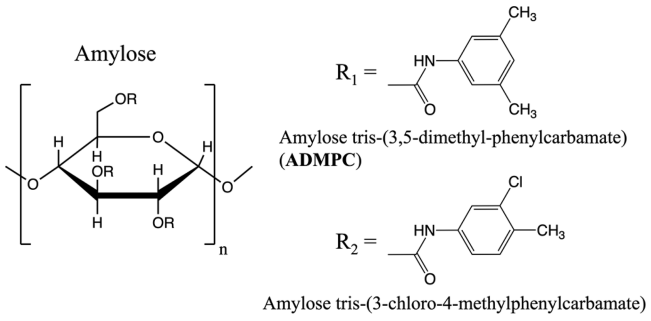

Figure 1. Structural representation of polysaccharide-based chiral stationary phase with an amylose backbone, with two examples of derivatives shown on the right.

The most prevalent consensus on the interaction mechanism between the CSPs and enantiomers is that at least three sites of interaction must be available to effect chiral discrimination, often referred to as the Easson-Stedman "three-point interaction" model.[35] It claims that the CSPs should have two hydrogen bond interactions and one $\pi-\pi$ interaction to differentiate the enantiomers; one enantiomer-CSP configuration (or conformation; we will use these two words interchangeably throughout the rest of the paper) could have three interactions but the other corresponding configuration could only have two interactions due to steric hindrance. The stronger-bound enantiomer will be more strongly retained in the column, therefore will elute later than the weaker-bound enantiomer. This three-point model considers that the chiral molecules can have interactions with the selectors from only one side, which might not hold true in general. Therefore, this model was further extended by Topiol and Sabio[36] to a four-contact point interaction model, which is also claimed to be the minimum requirement for chiral recognition by Bentley.[37] A recognition mechanism with a more general criterion was later proposed by Topiol, based on the differences between the distance matrices of chiral molecules and selectors.[38] Despite decades of concerns about the inadequacy of the simplistic three-point interaction model, it is still used for illustrative purposes, especially when the chiral selector is not a plane.[39] However, these limitations of the three-point model make it less useful when considering the chiral recognition mechanism of polysaccharide-based CSPs because of the additional hydrogen-bonding sites contributed by the derivatives on the polymer, and that the hydrogen-bonding sites in one derivative are on the same plane. Moreover, static configurational recognition models overlook the fact that chiral recognition is a dynamic process, in which the structure of CSPs and enantiomers change dynamically in the presence of the mobile phase.

The structure and the chiral recognition mechanism of the most widely used chiral stationary phases, polysaccharide-based CSPs, have been extensively investigated.[20,40−42] The structure of one typical example of polysaccharide-based CSPs often used as the model system is amylose tris(3,5-dimethyphenylcarbamate) (ADMPC), which has been scrutinized via many different experimental techniques, including solid state nuclear magnetic resonance spectroscopy (NMR),[43] NMR in solution using the 2D Nuclear Overhauser Enhancement (NOESY) technique,[44] vibrational circular dichroism (VCD),[45] and attenuated total reflection infrared spectroscopy (ATR-IR).[41] Yamamoto et al.[44] reported that ADMPC possesses a left-handed 4/3 helical structure in chloroform. Ma et al. used VCD measurements and also suggested a left-handed helical structure of ADMPC.[45] Similar conclusions were drawn by Wenslow and Wang using solid state NMR.[46] In the helical structure of ADMPC deduced from these observations, the glucose ring is regularly arranged along the axis; the carbamate groups are located inside the grooves of the polymer, while the phenyl groups are located outside the polymer chain, as shown in Figure 2. Besides the backbone helical structure, the structure of the side chain has also been studied and reported by Kasat et al.[47] that it has a planar conformation. Traditional models of the chiral recognition mechanism might not be easily adopted by polymer chiral selectors, because of the many potential interacting sites contributed by different derivatives, therefore

DOI: 10.1021/acs.langmuir.7b02337
Langmuir 2017, 33, 11246−11256

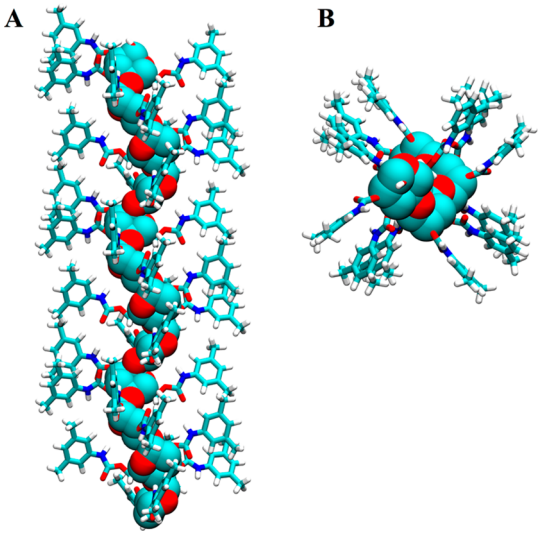

Figure 2. Structure of the initial configuration of ADMPC including a side view (A) and a top view (B). The backbone atoms are represented with VdW spheres and the derivatives are represented with sticks. Hydrogen atoms are in white, carbon atoms are in cyan, nitrogen atoms are in blue, and oxygen atoms are in red.

there is no single enantiomer-CSP structure in solid and solution states. Nevertheless, mechanisms of many enantioseparations using ADMPC have been proposed. Bereznitski et al.[48] suggested that the difference in the strengths of the hydrogen bonds formed between the enantiomer and the C═O group of ADMPC is the main reason for the enantioseparation based on differential scanning calorimetry (DSC) and ATR-IR. Ye et al.[49] reported that the nonbonded interaction energy, i.e., van der Waals (VdW) and electrostatic energy, between ADMPC and O-*tert*-butyltyrosine allyl ester in one enantiomer is stronger than the other, to which they attributed the chiral separation.

Computational chemistry and molecular modeling provide a closer look at the detailed structure of the chiral selectors and their interaction with enantiomers, which help to elucidate the chiral recognition mechanism of ADMPC. In combination with NMR experiments, Ye et al.[49] used implicit-solvent molecular dynamics (MD) simulations to study the interaction between a 12-mer of ADMPC with a fixed backbone and the enantiomers of *p*-O-*tert*-butyltyrosine allyl ester which were placed in the groove of ADMPC at the beginning of the simulation. Pair distribution functions generated from the simulation agree well with 2D NOESY spectra. However, their simulation lasted for 2 ns, which might not be long enough to reach equilibrium, and the fixed backbone structure and the placement of the enantiomers in the groove might also have caused some artifacts that could affect the results of the simulation. Furthermore, implicit solvent simulations do not take into account possible local contributions of solvent molecules to the configuration energy. Similar MD simulations have been reported by Kasat et al.,[41] which were also conducted on a system containing ADMPC with fixed backbone structure in the absence of solvent molecules. Li et al.[50] conducted molecular docking simulations as well as MD simulations of the interactions between an ADMPC with a fixed backbone dihedral angle and metalaxyl/benalaxyl enantiomers, and they concluded that hydrogen bonding is a key factor controlling the chiral separation. Unfortunately, the docking simulations were based on static configurations of ADMPC and enantiomers, thus missing the dynamic nature of the chiral recognition process in their studies. Density functional theory (DFT) calculations have also been employed to elucidate the binding mechanism between ADMPC and enantiomers. Tsui et al.[51] used DFT methods to study the interaction between the enantiomers and a single molecule of methyl *N*-methyl carbamate. They proposed a recognition mechanism with three-point interactions, a strong hydrogen bond between the enantiomer and the C═O group on a single molecule of carbamate, a weaker hydrogen bond between the enantiomer and the N−H group of the carbamate molecule, and an interaction involving the phenyl group based on the following respective energy-minimized structures: solute OH group placed next to C═O of the carbamate molecule, solute C═O next to NH of the carbamate. However, in reality the ADMPC polymer has a large number of glucose units and three carbamate side chains on each unit, thus having numerous potential hydrogen-bonding sites. The lowest energy configurations they considered may not be consistent with the lowest energy configuration of one enantiomer with the polymer in the presence of solvent molecules. We shall demonstrate the role of the solvent in developing the structure of the CSP in the present work.

The composition of the mobile phase can have a crucial effect on chiral recognition because it can affect the structure of the chiral selector and the enantiomer. The effect of the solvent has not been considered in previous theoretical computational studies or in any proposed mechanisms; however, there are indications that the mobile phase could play a role in chiral separations. Studies using solid state NMR have already shown that hexane, an often used mobile phase, becomes incorporated into the structure of the CSPs.[52] In addition, changing to a polar solvent in the mobile phase is found to change the structure of the CSPs by affecting the intra- and intermolecular hydrogen bonds.[52] From our recent experimental studies (to be published), we have observed that simply changing the mobile phase can have a significant effect on the separation of chiral drugs; in particular, the chromatographic separation of 2s-flavanone and 2r-flavanone, as shown in Figure 3, exhibits a

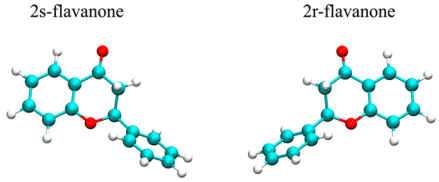

Figure 3. Molecular structure of flavanone enantiomers, 2s-flavanone (left) and 2r-flavanone (right). The molecules are depicted with ball-and-stick models with cyan beads representing carbon atoms, red beads representing oxygen atoms, and white beads for hydrogen atoms.

distinct change when the mobile phase is switched from methanol to heptane/IPA (90/10) solvent. Several MD simulations studies have shown that the absence of explicit solvent in the simulation might induce significant errors in the results of the simulation of the binding of ligands to proteins.[53] Therefore, inclusion of explicit solvent molecules is critical in MD simulations to provide a realistic presentation of the structural behavior of the CSPs and enantiomers and their interactions with each other.

DOI: 10.1021/acs.langmuir.7b02337
Langmuir 2017, 33, 11246−11256

In this Article, we applied explicit-solvent atomistic MD simulations to better understand experimentally observed solvent effects on the chiral recognition mechanism. Flavanone enantiomers, 2r-flavanone and 2s-flavanone, and ADMPC are used in this study to examine the different interactions they might have under the different solvent conditions used experimentally. This particular example arose from our experimental studies, in which we observed the large difference in separation factors upon changing only the mobile phases. More therapeutic examples will be investigated in our next study. Here, we focus on elucidating the solvent effect on the separation of enantiomers using ADMPC. We demonstrate the left-handed helical structure of ADMPC in MD simulations in different solvents, in agreement with NMR studies,[44] without imposing any restraints on the backbone dihedral angles or the backbone atom positions. We report the different configurations that ADMPC adopts in methanol and in heptane/IPA (90/10), which is further explained by the distribution of solvent molecules along the backbone of ADMPC. We observe differences in configuration in different solvent conditions for the polymer alone in solution. More importantly, we find quantitatively significant differences in the interactions between ADMPC and the flavanone enantiomers in the presence of the two solvent systems. These differences correlate with the experimental elution order of the two enantiomers for both solvent systems, as well as the experimental solvent effect on the separation factor. We present here the chiral recognition mechanism from a new and dynamic atomistic perspective.

METHOD

Generating Force Field Parameters for ADMPC and Flavanone. To obtain the partial charges for ADMPC, 2r-flavanone, and 2s-flavanone for our simulations using AMBER 14,[54] we performed quantum mechanical (QM) calculations using the GAUSSIAN09 software package. The structure of the flavanone is shown in Figure 3. To facilitate the QM calculations on ADMPC, the partial charges were calculated for one monomer and later applied to each monomer along the polymer chain. Methyl groups were used to cap each end of the monomer when generating the partial charges. The structure of the ADMPC was obtained from Okamoto et al.,[44] which is already an optimized structure. We used this structure to generate the coordinates for the ADMPC monomer for estimating the partial charges. DFT-B3LYP/6-31G(d) Method/Basis set combination was used for calculating partial charges of both ADMPC and flavanone enantiomers. Antechamber[54] in the Ambertools was then used to generate the force field parameters such as bond, angle, dihedral, and nonbonded energy terms based on the GAFF (General AMBER force field) parameter library.

Getting the Average Structure of ADMPC in Different Solvents. One 12-mer ADMPC chain was placed into the solvent box (containing either methanol or heptane/IPA (90/10 v/v)) to generate the average structure using clustering analysis. The average structures in the two solvent systems will later be used as the starting points when both ADMPC polymer and flavanone enantiomer are in the same simulation system. We used a $70 \times 70 \times 70$ Å^3 box, large enough to ensure that the 12-mer ADMPC does not interact with its periodic mirror image. Two types of simulations are performed: one contains one 12-mer ADMPC chain and 4826 methanol molecules, the other contains one 12-mer ADMPC polymer, 1159 heptane molecules, and 215 IPA molecules, to mimic the exact concentrations of the experimental conditions (based on the density of the solution, the molar mass of the solvent molecules, the composition of the mixture, and the size of the simulation box).

Each simulation was conducted at 298 K for 100 ns to permit the ADMPC polymer to approach equilibrium. The simulations contain the following steps as described in Zhao et al.[55,56] First, a solvent minimization was performed for 10 000 steps using the steepest descent method with the ADMPC chain restrained with a force of 10.0 kcal/mol. Then the system was gradually heated in 100 ps to reach the target temperature of 298 K with the ADMPC polymer restrained via a force of 10.0 kcal/mol. After that, an NPT ensemble MD run was performed for 20 ps with ADMPC still restrained with the same force. Subsequently, another round of minimization for 10000 steps with a restraint of 5.0 kcal/mol on the ADMPC polymer was conducted, which is followed by another 20 ps NPT ensemble MD run with ADMPC restrained. Then, the system was further minimized without any restraint for another 10000 steps, followed by a reheating to the target temperature (298 K) in 40 ps. Eventually, a production NPT ensemble MD run was conducted for 100 ns. The temperature of the system was maintained by the Berendsen thermostat.[57] Long-range electrostatic interactions were calculated by Partial mesh Ewald (PME) summation[58] with a 9 Å cutoff radius. A 1×10^{-5} tolerance for the Ewald convergence was used to calculate the nonbonded interactions. Bonds involving hydrogen atoms were constrained via the SHAKE algorithm.[59] Each simulation was carried out for at least 100 ns. Statistical analysis is based on the last 40−60 ns of the trajectories using Ambertools, VMD, NAMD, and in-house scripts. Likewise, the 2s and 2r flavanone molecules were equilibrated in the two solvents and the results examined for any conformational transformations. Since these are small molecules, only 50 ns were sufficient at 298 K to achieve equilibration in the solvents. The result of the 2s and 2r molecules should be the same since the solvents are achiral.

Simulating the Interaction of ADMPC and Flavanone in Different Solvents. A single ADMPC polymer, a single flavanone enantiomer (either 2r-flavanone or 2s-flavanone) and solvent molecules are included in the system to reproduce the concentration condition of the experiment. In the chromatographic separation experiment, the concentration of the drug sample is 1 mg/mL; the volume of injection is 0.2 μL in each experiment; the column size is 3 mm I.D. × 50 mm long; the amount of silica gel in the column is around 0.2 g. In addition, the loading level of the ADMPC polymers on the silica gel (i.e., the weight of ADMPC polymer to the weight of the silica gel) must also be controlled. Based on the experimental conditions mentioned above, we calculated the number of drug molecules corresponding to one 12-mer ADMPC chain and found that there is approximately only 1 drug molecule per 12-mer chain in the experiment. The enantiomer, either R or S configuration, is then randomly placed in the $70 \times 70 \times 70$ Å^3 box with the 12-mer ADMPC polymer, followed by the addition of solvent molecules using the Packmol program.[60] The number of solvent molecules in the simulation box is the same as that mentioned in the previous section of each system, since the addition of only one small drug molecule would not have a significant effect on the density of the solution. Overall, four types of simulations were performed, including ADMPC +2r-flavanone in methanol, ADMPC+2s-flavanone in methanol, ADMPC+2r-flavanone in heptane/IPA (90/10), and ADMPC+2s-flavanone in heptane/IPA (90/10). The simulation procedure is the same as mentioned in the previous section. Each simulation was performed for at least 100 ns at 298 K.

Clustering Analysis. Clustering analysis is a method to generate the structure that has the largest population over the course of the simulation.[61] Only backbone atoms are taken into consideration here because the sole purpose of this analysis is to see if our model is able to maintain the helical structure observed in NMR experiments.[44] The hierarchical agglomerative approach is used in the clustering analysis. The minimum distance between clusters is set as 3.0 Å. A cluster was generated from the analysis based on the distance between frames calculated via best-fit coordinate RMSD using atoms in the backbone of ADMPC. A single representative structure of ADMPC is then generated in methanol and in heptane/IPA (90/10) solvent conditions. This is used as the starting configuration in the simulations containing both ADMPC and flavanone enantiomers in the two solvents. The flavanone molecules are found to be relatively rigid in these solvents.

DOI: 10.1021/acs.langmuir.7b02337
Langmuir 2017, 33, 11246−11256

RESULTS AND DISCUSSION

a. The Left-Handed Helical Configurations of ADMPC Differ in Different Solvent Conditions. The configurations of ADMPC in different solvents have qualitatively the same left-handed helical nature as observed by NMR studies,[44] but its dimensions differ in different solvents. Representative structures of ADMPC in methanol (Figure 4A) and heptane/IPA (90/10) (Figure 4B) were generated using clustering analysis from the last 20 ns of the simulation on the system that has one ADMPC polymer and solvent molecules (details of the clustering analysis can be found in the method section). As can be seen in Figure 4, each molecule from top to bottom has pitches with four monomers in each pitch, which agrees well with the 4/3 left-handed helical structure reported by Yamamoto[44] using NMR with the 2D NOESY technique in chloroform solution. A significant finding in our MD simulations is that the average configuration of the 12-mer ADMPC in heptane/IPA (90/10) is longer than in methanol. End-to-end distance is used to quantify the difference in the length of the polymer in Table 1, in which the configuration of ADMPC in heptane/IPA (90/10) is more extended than in methanol by 4.6 Å. This observation is only an indication of structural changes in the polymer. Later, we examine the structural changes further in terms of the glycosidic dihedral angle maps.

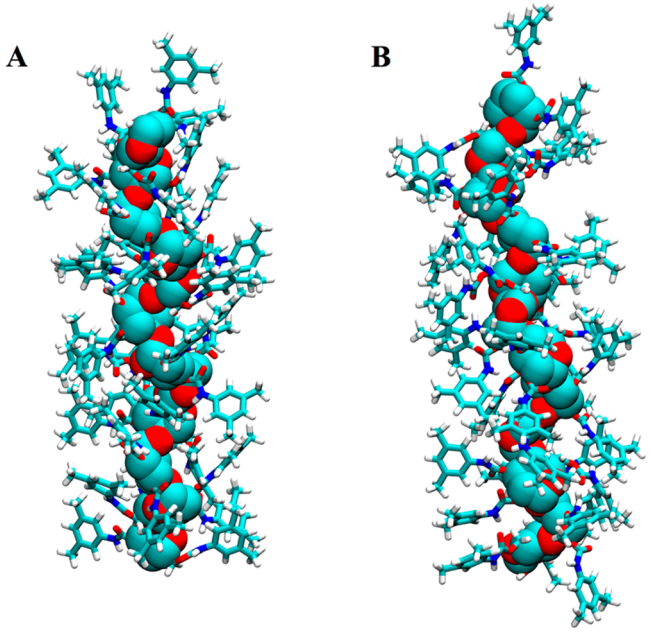

Figure 4. Average structures of ADMPC in methanol (A) and 90/10 Hep/IPA (B). The backbone atoms are represented with VdW spheres and the derivatives are represented with sticks. Hydrogen atoms are in white, carbon atoms are in cyan, nitrogen atoms are in blue, and oxygen atoms are in red.

Table 1. End-to-End Distance of the Average Structures of ADMPC in Different Solvents

solvent conditions	average of last 20 ns (Å)
methanol	35.25 ± 0.70
90/10 Hep/IPA	39.88 ± 0.96

To further quantify the helical structure of the ADMPC, the dihedral angles, φ (angle formed by $H_1-C_1-O-C_2$) and ψ (angle formed by $C_1-O-C_2-H_2$), involved in the glycoside bond[44] illustrated in Figure 5 are examined. These two angles determine the backbone helical structure of the ADMPC. In the experimental version, ADMPC is a much longer polymer and the end units are a very minor fraction of the total structure. Since a 12-mer ADMPC is under investigation in our system, only the glycoside bonds between adjacent monomers from the 2nd to the 11th were considered because the bonds that connect the terminal monomers are very flexible and do not contribute to the helical structure of ADMPC. The φ and ψ angles are then used as x and y axes to draw a probability map of the dihedral angles as shown in Figure 6, which is analogous to the Ramachandran plot[62] used in describing the secondary structure of polypeptides. The colors go from blue to red representing the density of points from low to high in various (φ, ψ) regions. As we can see from Figure 6A, the value of φ is mainly located between −30° and −90° and the value of ψ is located between −30° and −90°. We note, first of all, that the dynamic ADMPC polymer sweeps over a range of (φ, ψ) angles at 298 K. The most probable (φ, ψ) angles are around (−60°, −65°) in methanol. Similar to the dihedral angles in methanol, the dihedral angles of the glycoside bond between monomers of ADMPC in heptane/IPA (90/10) shown in Figure 6B also has the highest density region around (−58°, −65°). However, in addition, the dihedral angles in heptane/IPA (90/10) also show significant density in a new region around (−40°, −40°), indicating that the solvent makes a significant difference in the dihedral angles of the glycoside bond of ADMPC, thus leading to the length changes of the polymer. Yamamoto et al.[44] reported the dihedral angle for the glycoside bond in ADMPC in chloroform corresponding to the lowest energy is (−68.5°, −42.0°). In summary, many dihedral angles of the glycoside bond of ADMPC in both methanol and heptane/IPA (90/10) found from our simulations are located in the same quadrant as that in chloroform. However, dihedral angles populate slightly different regions in different solvents, indicating that the nature of the solvent affects the dynamic structure of the polymer. Note that the solvents used in our simulations are consistent with our experimental conditions. The NMR studies by Yamamoto used chloroform because the ADMPC can dissolve in it, hence the structure of ADMPC could be detected by NMR in solution. However, the ADMPC

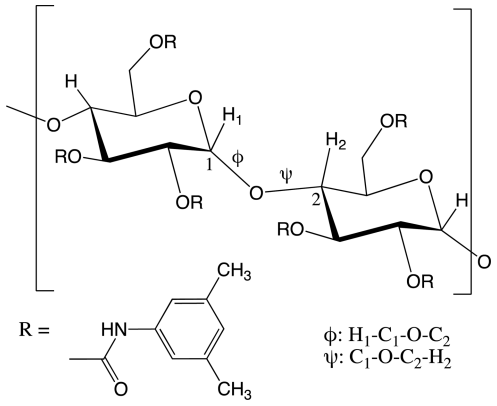

Figure 5. A representation of the dihedral angles of the glycoside bond between two adjacent monomers in ADMPC, including φ ($H_1-C_1-O-C_2$) and ψ ($C_1-O-C_2-H_2$).

DOI: 10.1021/acs.langmuir.7b02337
Langmuir 2017, 33, 11246−11256

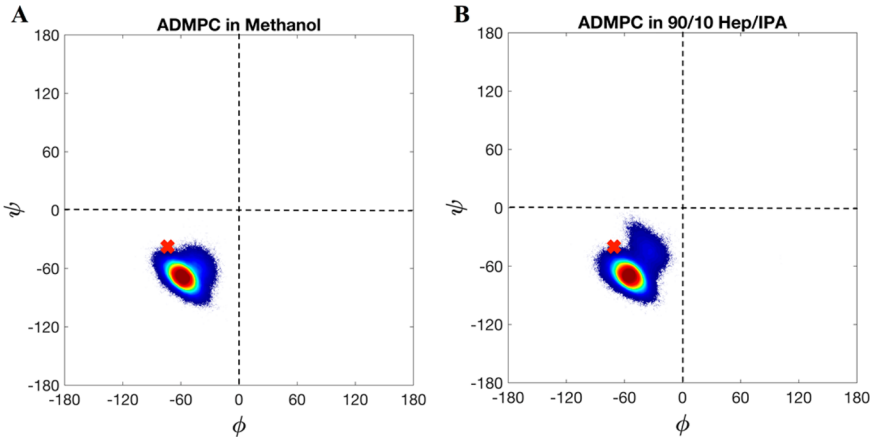

Figure 6. Maps of dihedral angles of the glycoside bond between adjacent monomers in methanol (A) and 90/10 Hep/IPA (B). The colors from blue to red represent the density of the data points going from low to high. The (φ, ψ) space is divided into 4 quadrants. The dihedral angles of the lowest energy structure of ADMPC obtained in chloroform are labeled as red exes.

polymers in the column we used in our experiments are coated onto the silica gel, which could leach off the silica support if the mobile phase is too strong, such as chloroform.

b. Solvent Molecules Distribute Differently around the ADMPC Chain. Different solvent molecules are found to behave differently close to ADMPC, indicated by averaging the radial distribution functions (RDF) of the center of mass of the solvent molecule to each atom on the backbone of ADMPC, as shown in Figure 7. The RDF curves are calculated using the last

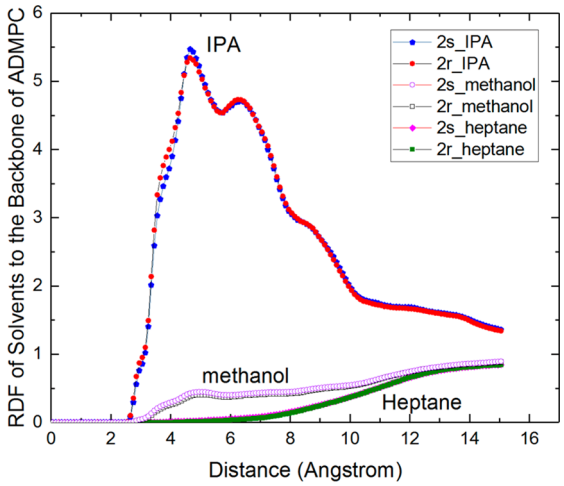

Figure 7. Radial distribution function of the center of mass of the solvent molecule to the backbone of ADMPC in methanol and heptane/IPA (90/10) (B). RDF curves obtained in the system containing 2r-flavanone and the system containing 2s-flavanone are both displayed.

60 ns of the trajectories of the simulations containing one ADMPC polymer, either a 2s-flavanone or 2r-flavanone molecule, and solvent molecules. The RDF curves of methanol to the backbone of ADMPC (Figure 7A) shows a shoulder around 5 Å, indicating a small attractive well for methanol molecules close to the backbone of ADMPC. There is a slightly greater probability for the system containing 2s-flavanone than that containing 2r-flavanone (0.44 vs 0.42), indicating that the solvent behaves differently with different enantiomers interacting with the ADMPC in the system, i.e., the methanol molecules are slightly closer to ADMPC when the latter is interacting with the 2s-flavanone. In experiments, we found that 2r-flavanone is the first to elute from the column, meaning that 2s-flavanone is more favorably interacting with ADMPC.

On the other hand, the IPA and heptane molecules behave completely differently compared with each other and with methanol. The RDF curve of IPA molecules has a peak at around 4.65 Å, which is closer than that of methanol. Moreover, the height of the peak, ~ 5.5, is much higher than that of methanol, which is 0.45. This indicates that IPA molecules have a significantly higher density at an even closer distance to the backbone of ADMPC than do the methanol molecules. This finding is counterintuitive since IPA molecules are the minority in the system of heptane/IPA (90/10) and the polarity of the IPA molecule is lower than that of the methanol molecules. The distribution behavior of the heptane molecules is of great importance to understand the behavior of IPA molecules in this system. The RDF curves of heptane molecules have a low probability of being found in close proximity to the backbone atoms of ADMPC; the region of space close to the backbone of ADMPC is almost fully occupied by IPA molecules, with the exclusion of heptane molecules. The RDF curves reveal that IPA molecules are pressed against the backbone of ADMPC by heptane molecules. This might also explain why the configurations taken by ADMPC (in terms of the dihedral angles of glycoside) behave differently in methanol and in heptane/IPA (90/10). As in methanol, the peak of the RDF curves of IPA molecules in the system containing 2s-flavanone is slightly higher than that containing 2r-flavanone (5.5 vs 5.4), i.e., the IPA molecules are slightly closer to ADMPC when the latter is interacting with 2s-flavanone, compared with 2r-flavanone.

c. Solvent Molecules Are Involved in the Interaction between the Chiral Drug and ADMPC. Solvent molecules are found to play a critical role in the interaction between chiral drugs and ADMPC, which is revealed by the correlation between the drug-ADMPC electrostatic interaction energy and the number of solvent molecules within 5 Å of the flavanone enantiomers. As can be seen from Figure 8A,C,E,G, the electrostatic energy between flavanone and ADMPC has various clusters along the time series, indicating multiple times of interactions between flavanone and ADMPC. For the times when flavanone and ADMPC have interaction energies strongly attractive enough, a decrease in the number of solvent

DOI: 10.1021/acs.langmuir.7b02337
Langmuir 2017, 33, 11246−11256

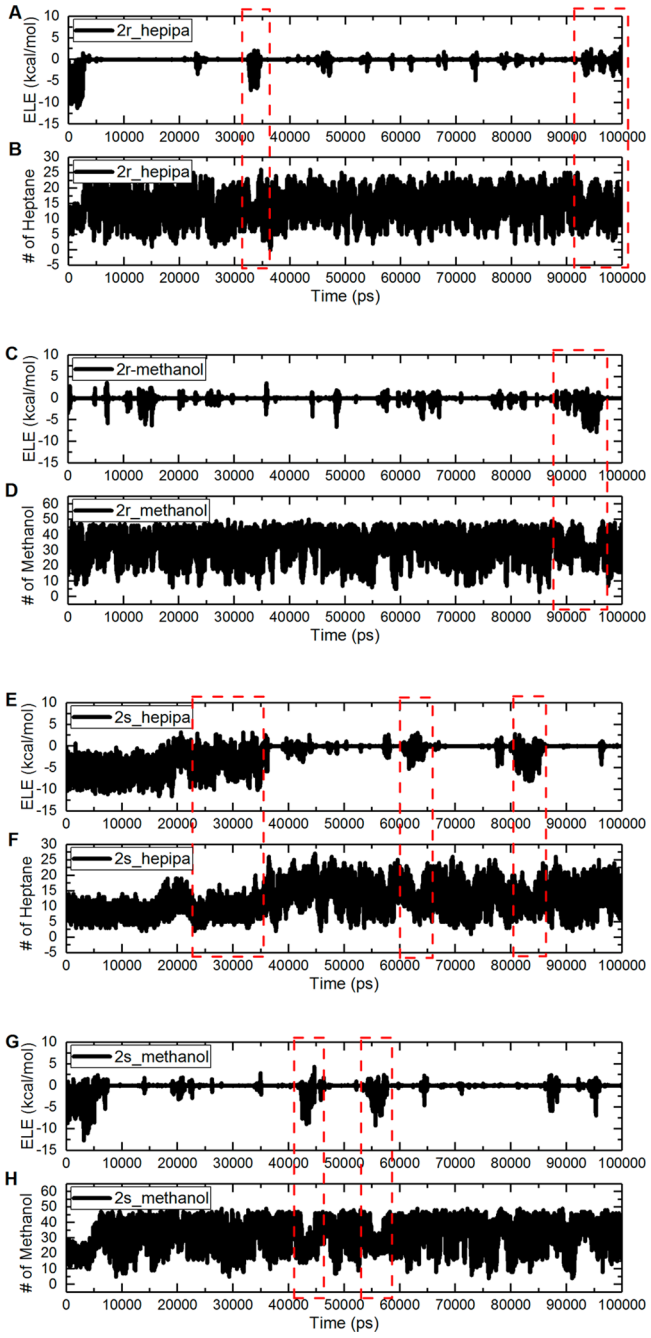

Figure 8. Electrostatic energies between flavanone isomers and ADMPC (A,C,E,G) and the number of solvent molecules in the first solvation layer of the drug over simulation time (B,D,F,H). The time frames where there is a correlation between electrostatic energy and the number of solvent molecules are enclosed in red dashed rectangles. Note the difference in scale between (B,F) and (D,H).

molecules around the drug is also observed. This correlation can be found in the systems with flavanone enantiomers and methanol. A similar correlation can be found between the number of heptane molecules and the electrostatic energy between flavanone and ADMPC in the system with heptane/IPA (90/10) molecules.

The rationale for choosing the properties noted above to investigate are as follows: Only the electrostatic interaction energy between flavanone and ADMPC is considered because the mechanism of chiral recognition strongly depends on the hydrogen bonding interaction, which is included in the electrostatic interaction. Another reason is that the VdW interaction energy has not been found to have any correlation with the selectivity in this system. We only present the number of heptane molecules versus the time in the system with heptane/IPA (90/10) because the correlations between the number of IPA molecules and the electrostatic energy between the drug and ADMPC are hard to see, given that the number of IPA molecules is much lower than that of the heptane molecules. Note that in the case of the heptane/IPA solvent systems, we have seen that the IPA molecules have a much higher probability of being found close to the ADMPC backbone than the heptane molecules. However, this does not mean that heptane molecules play no role in the interaction between flavanone and ADMPC. This is because flavanone enantiomers will have a much higher probability of being solvated by heptane molecules than IPA molecules before it interacts with the ADMPC. At the same time that flavanone enantiomers interact with ADMPC, a significant drop in the number of heptane molecules, within the solvation distance occurs, but not in the IPA molecules, which also explains why we are not able to see a correlation between the number of IPA molecules close to flavanone enantiomers and the electrostatic ADMPC−flavanone interactions.

d. Selectivity Can Be Correlated with the Lifetime of H-Bonding between the Drug and ADMPC. Since hydrogen-bonding is an important component of the interaction energy between the flavanone enantiomers and the ADMPC polymer, we carried out a hydrogen-bonding analysis of our MD simulation results. Hydrogen bonding analysis was conducted based on a donor−acceptor distance cutoff of 3.5 Å and an angle cutoff of 30° away from linearity. For this analysis, the lifetime of hydrogen bonds is defined as the length of time that a specific hydrogen bond remains "present". In our simulation, we count a pair of atoms forming hydrogen bonds with each other as 1, otherwise 0. For example, if we get a time series data set of 10 frames as {1 1 0 1 1 1 1 0 0 1} for a specific pair of donor−acceptor atoms that are forming a hydrogen bond with each other, the overall fraction present will be designated as 0.7. However, there are three lifetimes observed, viz., 2, 4, and 1. The maximum lifetime is therefore 4, and the average lifetime is 3.5, i.e. (2 + 4+1)/3 = 3.5. The hydrogen bond forms three times in these 10 frames of time, and the total frames in which hydrogen bonds formed is 7. All the potential hydrogen-bonded pairs are monitored and recorded throughout the simulations. A time series of all the hydrogen bonded pairs are then generated. Three quantities are calculated for each pair, the maximum lifetime, the average lifetime, and the number of the total frames of the hydrogen bonds within the time frames under investigation. After that, both the maximum and the average of each quantity for all the hydrogen-bonded pairs are calculated and presented in Table 2. The ratios of all the values between 2r-flavanone and 2s-flavanone in methanol solvent are also presented in Table 2.

As can be seen from Table 2, all the values related to the hydrogen bonding lifetime between 2r-flavanone and ADMPC are smaller than those between 2s-flavanone and ADMPC. Therefore, all the values for the ratio of 2*r*/2s are less than 1. This indicates that the lifetime of the hydrogen bonds formed between 2r-flavanone and ADMPC is shorter than that between 2s-flavanone and ADMPC. Therefore, ADMPC prefers 2s-flavanone over 2r-flavanone, based on what we found in the simulation, which agrees well with the experimental observation

DOI: 10.1021/acs.langmuir.7b02337
Langmuir 2017, 33, 11246−11256

Table 2. Maximum Values, Average Values, and the Ratio of These Values between 2r and 2s of the Hydrogen-Bonding-Lifetime-Related Properties between the Drug and the ADMPC in Methanol

methanol	MaxLT[a]	AvgLT[b]	HBFrames[c]
2s			
max[d]	41	5.80	719
average[e]	15.5 ± 4.44	3.25 ± 0.52	210.5 ± 84.99
2r			
max	10	2.2	82
average	7 ± 0.63	1.88 ± 0.06	32.8 ± 6.31
ratio (2r/2s)			
max	0.24	0.38	0.11
average	0.46	0.58	0.16

[a]MaxLT represents the maximum lifetime of a hydrogen bond. [b]AvgLT stands for the average lifetime of a hydrogen bond. [c]HBFrames is the total number of frames that a hydrogen bond exists throughout the entire trajectory of the simulation. [d]Max is the maximum value of the properties (MaxLT, AvgLT, HBFrames) over all the possible hydrogen bonds in the system. [e]average is the average value of the properties (MaxLT, AvgLT, HBFrames) over the number of all the possible hydrogen bonded atom pairs in the system.

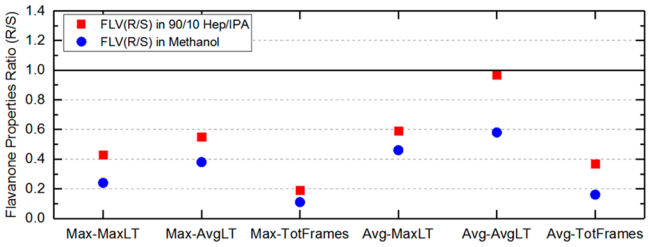

Figure 9. Ratio of hydrogen-bonding-lifetime-related quantities of 2r-flavanone and 2s-flavanone (2r/2s). The black solid line represents a ratio of 1.

that 2r-flavanone elutes first in the chromatogram and 2s-flavanone elutes last. Note that the "HBframes" in Table 2 stands for the total number of frames in which appropriate H-bond formed between enantiomer and CSP are found, which is different than the total number of frames (the entire MD trajectory) used to examine the maximum and average values of each hydrogen-bonding-lifetime-related properties.

The selectivity, a quantity in chromatography that characterizes the retention difference between the two species of interest, of 2r-flavanone over 2s-flavanone observed from experiments is 0.4 in methanol. All the parameters describing the hydrogen-bonding lifetimes in methanol give a ratio 2r/2s less than 1, that is, all correlate with the experimentally determined elution order. However, of these parameters, both the ratios of the maximum of the average lifetime of hydrogen bonds formed between flavanone and ADMPC (0.38), and the average of the maximum lifetime between flavanone and ADMPC (0.46), are close to 0.4. In summary, the ratios of the hydrogen-bonding lifetime-related properties reflect well the selectivity of the flavanone enantiomers obtained in experiments.

e. The Solvent Effect Can Also Be Captured by the Lifetime of the Hydrogen Bonds between Flavanone and ADMPC. The properties related to the lifetime of the hydrogen bonds formed between the flavanone enantiomers and ADMPC are found to capture the experimentally observed solvent effect on selectivity, as shown in Figure 9. First, all the values reflect the correct selectivity, that is, the ADMPC prefers 2s-flavanone over 2r-flavanone no matter what solvent system it is in, which can be seen from Figure 9 in that all the values are below 1.0. At the same time, we found all the values in methanol are lower than the corresponding values in heptane/IPA (90/10); in other words, all the values in heptane/IPA (90/10) are closer to 1.0 than those in methanol. This indicates that the selectivity of the flavanone enantiomers is weaker in heptane/IPA (90/10) than in methanol, which matches the experimental observations: The selectivity of 2r-flavanone over 2s-flavanone observed from experiments is 0.4 in methanol and 0.97 in heptane/IPA (90/10). All the hydrogen-bonding-lifetime-related properties qualitatively agree with the experimental observation.

The hydrogen-bonding-lifetime-related properties reflect the dynamic nature of the chiral recognition mechanism. They are able to reproduce not only the selectivity but also the solvent effects on the selectivity. Different from previous computational approaches in which partially fixed structures of chiral selector were used, this study does not impose any constraints or restraints on the structures of any of the molecules involved. Therefore, the entire dynamic nature of the process of the interaction between flavanone enantiomers and ADMPC in the presence of solvent can be observed at the level of atomistic detail, which also means that hydrogen bonds can be observed to be forming and breaking multiple times between the drug enantiomers and a freely moving ADMPC chain. Additional drug enantiomers are under investigation in MD simulations to find out the best criterion among the hydrogen-bonding-related-properties that can be correlated with experimental observations. For the present, with this example, we have found consistency with experimental results. A more detailed analysis of the distribution of hydrogen-bonding lifetimes of specific H-bonds will be carried out in a future study, where we consider many more examples of enantiomer pairs with the same CSP and comparisons between them can be made.

It is important to note that no single static picture correlates with the experimental elution order or selectivity; neither the minimum energy configuration nor the greatest interaction energy. Therefore, theoretical treatments that consider one or even both of these cannot be expected to reproduce the solvent effect.

To complete the picture, we carried out a statistical analysis of the π stacking arrangements, since $\pi-\pi$ interactions have been suggested as the necessary third component in the three-point chiral recognition models. The flavanone has three rings, one has some freedom to rotate relative to the two fused rings. Each of the rings in flavonone could interact with the rings projecting out of the ADMPC backbone. Our statistical analysis of the π stacking lifetimes are carried out using the same strategy as the hydrogen bonding lifetime analysis. The results, based on the π stacking experienced by the phenyl ring in flavanone (that has a rotational degree of freedom) with the rings of the ADMPC, seem to indicate higher average numbers for the 2s enantiomer compared to the 2r in all properties except the average of the average lifetimes. The latter is either nearly the same (for a distance cutoff of 4.5 Å) or is shorter for the 2s (for a distance cutoff of 4.0 Å). Thus, π stacking appears to contribute somewhat to the discrimination between 2s and 2r, but is, by itself, not sufficient to provide a basis for the separation. Obviously, the steric effects posed by the rings either facilitate or hinder the hydrogen-bonding interactions

DOI: 10.1021/acs.langmuir.7b02337
Langmuir 2017, 33, 11246−11256

between the flavanone enantiomers and the ADMPC, but any arrangements that could contribute favorably to the energy via a π stacking interaction do not appear to dominate energetically to influence the elution order.

The picture that emerges from the MD simulations is that, in the presence of the solvent, hydrogen-bonding correlations are dynamically formed and broken over and over as each enantiomer moves along the column. The interactions between the s and r molecules and the ADMPC chain are intrinsically different, thus leading to different dynamics of the hydrogen bond formation with the longer-lived hydrogen bonds contributing the most to the retention of one enantiomer over another.

CONCLUSIONS

Explicit-solvent atomistic molecular dynamics simulations were performed on a system with a free ADMPC chain, flavanone enantiomers, and either methanol or heptane/IPA (90/10) solvent molecules to elucidate the chiral recognition mechanism on polysaccharide-based chiral stationary phases. The model of ADMPC was validated under different solvent conditions, in that it maintains the left-handed 4/3 helical structure, which was observed in NMR studies in solution.[44] The ADMPC polymer in methanol was found to have a different configuration from that in heptane/IPA (90/10), in that the length of the ADMPC in methanol is shorter than in heptane/IPA (90/10). Furthermore, it was found that dihedral angles of the glycoside bond of ADMPC in heptane/IPA (90/10) have a wider distribution than in methanol, indicating that the solvent molecules have a significant effect on the dihedral angle of the glycoside bond of ADMPC, leading to the polymer have different average lengths in the different solvents.

Moreover, the radial distribution function of the solvent molecules relative to the backbone of the ADMPC polymer reveals that different solvent molecules are distributed differently around the backbone of the ADMPC. The RDF of methanol to the backbone of ADMPC polymer has a slight peak around 5.0 Å at approximately the same distance as the peak in the RDF of IPA in the heptane/IPA (90/10) environment. However, the height of the peak of the RDF of IPA is significantly higher than that of methanol even though the number of molecules of IPA in the simulation system is much fewer than the number of methanol molecules in the pure methanol case, that is, most of the IPA molecules stay close to the ADMPC backbone throughout the simulations. At the same time, there is low probability of finding heptane in the immediate vicinity of the ADMPC backbone. The RDF curves indicate that all the IPA molecules are essentially being pressed against the backbone of ADMPC by heptane molecules. Therefore, the changes in the dihedral angle of the glycoside bond in the heptane/IPA (90/10) system is mainly contributed by the IPA molecule, although the heptane, through hydrophobic interactions with one another cause the IPA molecules to crowd closer to the backbone of ADMPC to facilitate this. Note that this is the first study showing the dynamic nature of the atomic-level changes in the structure of the chiral stationary phase due to the mobile phase, and how such changes in structure differ from one solvent system to another.

The number of solvent molecules around the enantiomer of flavanone was found to correlate well with the interaction between the ADMPC and the enantiomer of flavanone in terms of electrostatic interaction energy. The number of solvent molecules within 5 Å of the drug molecule significantly decreases when the drug molecule interacts with the ADMPC polymer. In the absence of the ADMPC, the enantiomers form hydrogen bonds within the methanol or IPA, or hydrophobic interactions with the hexane, forming a stable first solvation shell. Preferential hydrogen bonding with the chiral stationary phase, which is dynamic but in a limited way (unlike the individual solvent molecules which can translate throughout the box), means shedding some of the coordinated solvent molecules. This may be the reason for the correlation throughout the MD trajectory, of fewer coordinated solvent molecules time-coincident with strong enantiomer-CSP interactions. Hydrogen bonding analysis reveals the basis for selectivity: The lifetime of the hydrogen bonds formed between the flavanone enantiomer and ADMPC polymers is found to correlate well with the selectivity of the enantiomers. The 2s-flavanone has a longer hydrogen-bonding lifetime with ADMPC than 2r-flavanone, which agrees well with the longer retention time of 2s-flavanone on the column in experiments. Finally, the lifetime of hydrogen bonds formed between flavanone enantiomers and ADMPC changes in different solvents. The ratio of the hydrogen-bonding-lifetime-related properties is closer to 1.0 in heptane/IPA (90/10) than in methanol, indicating the selectivity in heptane/IPA (90/10) is weaker than that in methanol. This, too, matches the experimental observations of selectivity factors 0.9 and 0.4, respectively. Further drug enantiomers need to be screened via MD simulations to discern which properties related to the hydrogen bonding lifetimes best reproduce the actual lab results for most enantiomer pairs, as well as for different chiral stationary phases and mobile phases. Our analysis of the $\pi-\pi$ interactions do not reveal a correlation with elution order or separation factor; however, steric effects involving the planar rings of the solute and the chiral selector clearly do play an important role in determining the probabilities of the configurations that facilitate the hydrogen bonding interactions that do correlate with elution order and separation factor. Eventually the computational approach adopted here can be used as a prescreening tool for choosing the experimental conditions for optimum chiral molecular separation.

AUTHOR INFORMATION

Corresponding Author

*E-mail: murad@iit.edu.

ORCID

Sohail Murad: 0000-0002-1486-0680

Notes

The authors declare no competing financial interest.

ACKNOWLEDGMENTS

Financial support from the National Science Foundation (under Grants SBIR 1621012 and CBET 1545560).

REFERENCES

(1) Nguyen, L. A.; He, H.; Pham-Huy, C. Chiral Drugs: an Overview. *Int. J. Biomed. Sci.* **2006**, *2*, 85−100.

(2) Cahn, R. S.; Ingold, C.; Prelog, V. Specification of Molecular Chirality. *Angew. Chem., Int. Ed. Engl.* **1966**, *5*, 385−415.

(3) Arnesano, F.; Pannunzio, A.; Coluccia, M.; Natile, G. Effect of Chirality in Platinum Drugs. *Coord. Chem. Rev.* **2015**, *284*, 286−297.

(4) Iacopetta, D.; Carocci, A.; Sinicropi, M. S.; Catalano, A.; Lentini, G.; Ceramella, J.; Curcio, R.; Caroleo, M. C. Old Drug Scaffold, New Activity: Thalidomide-Correlated Compounds Exert Different Effects

DOI: 10.1021/acs.langmuir.7b02337
Langmuir 2017, 33, 11246−11256

on Breast Cancer Cell Growth and Progression. *ChemMedChem* **2017**, *12*, 381−389.
(5) Kenyon, B. M.; Browne, F.; D'Amato, R. J. Effects of Thalidomide and Related Metabolites in a Mouse Corneal Model of Neovascularization. *Exp. Eye Res.* **1997**, *64*, 971−978.
(6) Tseng, S.; Pak, G.; Washenik, K.; Keltz Pomeranz, M.; Shupack, J. L. Rediscovering Thalidomide: a Review of Its Mechanism of Action, Side Effects, and Potential Uses. *J. Am. Acad. Dermatol.* **1996**, *35*, 969−979.
(7) Schurig, V. Gas Chromatographic Enantioseparation of Derivatized A-Amino Acids on Chiral Stationary Phases–Past and Present. *J. Chromatogr. B: Anal. Technol. Biomed. Life Sci.* **2011**, *879*, 3122−3140.
(8) Xie, S.-M.; Yuan, L.-M. Recent Progress of Chiral Stationary Phases for Separation of Enantiomers in Gas Chromatography. *J. Sep. Sci.* **2017**, *40*, 124−137.
(9) Fanali, C.; Fanali, S.; Chankvetadze, B. HPLC Separation of Enantiomers of Some Flavanone Derivatives Using Polysaccharide-Based Chiral Selectors Covalently Immobilized on Silica. *Chromatographia* **2016**, *79*, 119−124.
(10) Jibuti, G.; Mskhiladze, A.; Takaishvili, N.; Karchkhadze, M.; Chankvetadze, L.; Farkas, T.; Chankvetadze, B. HPLC Separation of Dihydropyridine Derivatives Enantiomers with Emphasis on Elution Order Using Polysaccharide-Based Chiral Columns. *J. Sep. Sci.* **2012**, *35*, 2529−2537.
(11) Merola, G.; Fu, H.; Tagliaro, F.; Macchia, T.; McCord, B. R. Chiral Separation of 12 Cathinone Analogs by Cyclodextrin-Assisted Capillary Electrophoresis with UV and Mass Spectrometry Detection. *Electrophoresis* **2014**, *35*, 3231−3241.
(12) Orlandini, S.; Pasquini, B.; Del Bubba, M.; Pinzauti, S.; Furlanetto, S. Quality by Design in the Chiral Separation Strategy for the Determination of Enantiomeric Impurities: Development of a Capillary Electrophoresis Method Based on Dual Cyclodextrin Systems for the Analysis of Levosulpiride. *J. Chromatogr. A* **2015**, *1380*, 177−185.
(13) Preiss, L. C.; Werber, L.; Fischer, V.; Hanif, S.; Landfester, K.; Mastai, Y.; Munoz-Espi, R. Amino-Acid-Based Chiral Nanoparticles for Enantioselective Crystallization. *Adv. Mater.* **2015**, *27*, 2728−2732.
(14) Robl, S.; Gou, L.; Gere, A.; Sordo, M.; Lorenz, H.; Mayer, A.; Pauls, C.; Leonhard, K.; Bardow, A.; Seidel-Morgenstern, A.; et al. Chiral Separation by Combining Pertraction and Preferential Crystallization. *Chem. Eng. Process.* **2013**, *67*, 80−88.
(15) Ahuja, S. *Chromatography and Separation Science*; Academic Press: Cambridge, MA, 2003.
(16) Pirkle, W. H.; Finn, J. M.; Schreiner, J. L.; Hamper, B. C. A Widely Useful Chiral Stationary Phase for the High-Performance Liquid Chromatography Separation of Enantiomers. *J. Am. Chem. Soc.* **1981**, *103*, 3964−3966.
(17) Blum, A. M.; Lynam, K. G.; Nicolas, E. C. Use of a New Pirkle-Type Chiral Stationary Phase in Analytical and Preparative Subcritical Fluid Chromatography of Pharmaceutical Compounds. *Chirality* **1994**, *6*, 302−313.
(18) Suzuki, T.; Timofei, S.; Iuoras, B. E.; Uray, G.; Verdino, P.; Fabian, W. M. F. Quantitative Structure−Enantioselective Retention Relationships for Chromatographic Separation of Arylalkylcarbinols on Pirkle Type Chiral Stationary Phases. *J. Chromatogr. A* **2001**, *922*, 13−23.
(19) Addadi, K.; Sekkoum, K.; Belboukhari, N.; Cheriti, A.; Aboul-Enein, H. Y. Screening Approach for Chiral Separation of B-Aminoketones by HPLC on Various Polysaccharide-Based Chiral Stationary Phases. *Chirality* **2015**, *27*, 332−338.
(20) Chankvetadze, B. Recent Developments on Polysaccharide-Based Chiral Stationary Phases for Liquid-Phase Separation of Enantiomers. *J. Chromatogr. A* **2012**, *1269*, 26−51.
(21) Jibuti, G.; Mskhiladze, A.; Takaishvili, N.; Karchkhadze, M.; Chankvetadze, L.; Farkas, T.; Chankvetadze, B. HPLC Separation of Dihydropyridine Derivatives Enantiomers with Emphasis on Elution Order Using Polysaccharide-Based Chiral Columns. *J. Sep. Science* **2012**, *35*, 2529−2537.
(22) Stalcup, A. M.; Chang, S. C.; Armstrong, D. W.; Pitha, J. (S)-2-Hydroxyprophyl-B-Cyclodextrin, a New Chiral Stationary Phase for Reversed-Phase Liquid Chromatography. *J. Chromatogr. A* **1990**, *513*, 181−194.
(23) Pang, L.; Zhou, J.; Tang, J.; Ng, S.-C.; Tang, W. Evaluation of Perphenylcarbamated Cyclodextrin Clicked Chiral Stationary Phase for Enantioseparations in Reversed Phase High Performance Liquid Chromatography. *J. Chromatogr. A* **2014**, *1363*, 119−127.
(24) Ha, J. J.; Han, H. J.; Kim, H. E.; Jin, J. S.; Jeong, E. D.; Hyun, M. H. Development of an Improved Ligand Exchange Chiral Stationary Phase Based on Leucinol for the Resolution of Proton Pump Inhibitors. *J. Pharm. Biomed. Anal.* **2014**, *100*, 88−93.
(25) Ma, D. H.; Jin, J. S.; Jeong, E. D.; Hyun, M. H. Effect of the Residual Silanol Group Protection on the Liquid Chromatographic Resolution of A-Amino Acids and Proton Pump Inhibitors on a Ligand Exchange Chiral Stationary Phase. *J. Sep. Sci.* **2013**, *36*, 1349−1355.
(26) Tachibana, K.; Ohnishi, A. Reversed-Phase Liquid Chromatographic Separation of Enantiomers on Polysaccharide Type Chiral Stationary Phases. *J. Chromatogr. A* **2001**, *906*, 127−154.
(27) Shen, J.; Ikai, T.; Okamoto, Y. Synthesis and Application of Immobilized Polysaccharide-Based Chiral Stationary Phases for Enantioseparation by High-Performance Liquid Chromatography. *J. Chromatogr. A* **2014**, *1363*, 51−61.
(28) Shen, J.; Okamoto, Y. Efficient Separation of Enantiomers Using Stereoregular Chiral Polymers. *Chem. Rev.* **2016**, *116*, 1094−1138.
(29) Okamoto, Y.; Kaida, Y. Resolution by High-Performance Liquid Chromatography Using Polysaccharide Carbamates and Benzoates as Chiral Stationary Phases. *J. Chromatogr. A* **1994**, *666*, 403−419.
(30) Tang, Y. Significance of Mobile Phase Composition in Enantioseparation of Chiral Drugs by HPLC on a Cellulose-Based Chiral Stationary Phase. *Chirality* **1996**, *8*, 136−142.
(31) Lin, J. M.; Nakagama, T.; Uchiyama, K.; Hobo, T. Temperature Effect on Chiral Recognition of Some Amino Acids with Molecularly Imprinted Polymer Filled Capillary Electrochromatography. *Biomed. Chromatogr.* **1997**, *11*, 298−302.
(32) Jönsson, S.; Schön, A.; Isaksson, R.; Pettersson, C.; Pettersson, G. An Unexpected Temperature Effect Obtained on Enantiomer Separation Using CBH I-Silica as a Chiral Stationary Phase: Increase in Retention and Enantioselectivity at Elevated Column Temperature: a Chromatographic and Microcalorimetric Study. *Chirality* **1992**, *4*, 505−508.
(33) Haginaka, J.; Wakai, J.; Takahashi, K.; Yasuda, H.; Katagi, T. Chiral Separation of Propranolol and Its Ester Derivatives on an Ovomucoid-Bonded Silica: Influence of pH, Ionic Strength and Organic Modifier on Retention, Enantioselectivity and Enantiomeric Elution Order. *Chromatographia* **1990**, *29*, 587−592.
(34) Guo, Y.; Gaiki, S. Retention and Selectivity of Stationary Phases for Hydrophilic Interaction Chromatography. *J. Chromatogr. A* **2011**, *1218*, 5920−5938.
(35) Easson, L. H.; Stedman, E. Studies on the Relationship Between Chemical Constitution and Physiological Action: Molecular Dissymmetry and Physiological Activity. *Biochem. J.* **1933**, *27*, 1257−1266.
(36) Topiol, S.; Sabio, M. Interactions Between Eight Centers Are Required for Chiral Recognition. *J. Am. Chem. Soc.* **1989**, *111*, 4109−4110.
(37) Bentley, R. Diastereoisomerism, Contact Points, and Chiral Selectivity: a Four-Site Saga. *Arch. Biochem. Biophys.* **2003**, *414*, 1−12.
(38) Topiol, S. A General Criterion for Molecular Recognition: Implications for Chiral Interactions. *Chirality* **1989**, *1*, 69−79.
(39) Lämmerhofer, M. Chiral Recognition by Enantioselective Liquid Chromatography: Mechanisms and Modern Chiral Stationary Phases. *J. Chromatogr. A* **2010**, *1217*, 814−856.
(40) Ye, Y. Chiral Discrimination Study for Polysaccharide-Based Chiral Stationary Phases. In *Chiral Separation Methods for Pharmaceutical and Biotechnological Products*; John Wiley & Sons, Inc.: New York, 2011; pp 147−191.
(41) Kasat, R. B.; Franses, E. I.; Wang, N.-H. L. Experimental and Computational Studies of Enantioseparation of Structurally Similar

DOI: 10.1021/acs.langmuir.7b02337
Langmuir 2017, 33, 11246−11256

Chiral Compounds on Amylose Tris(3,5-Dimethylphenylcarbamate). *Chirality* **2010**, *22*, 565−579.
(42) Ikai, T.; Okamoto, Y. Structure Control of Polysaccharide Derivatives for Efficient Separation of Enantiomers by Chromatography. *Chem. Rev.* **2009**, *109*, 6077−6101.
(43) Hellriegel, C.; Skogsberg, U.; Albert, K.; Lämmerhofer, M.; Maier, N. M.; Lindner, W. Characterization of a Chiral Stationary Phase by HR/MAS NMR Spectroscopy and Investigation of Enantioselective Interaction with Chiral Ligates by Transferred NOE. *J. Am. Chem. Soc.* **2004**, *126*, 3809−3816.
(44) Yamamoto, C.; Yashima, E.; Okamoto, Y. Structural Analysis of Amylose Tris(3,5-Dimethylphenylcarbamate) by NMR Relevant to Its Chiral Recognition Mechanism in HPLC. *J. Am. Chem. Soc.* **2002**, *124*, 12583−12589.
(45) Ma, S.; Shen, S.; Lee, H.; Eriksson, M.; Zeng, X.; Xu, J.; Fandrick, K.; Yee, N.; Senanayake, C.; Grinberg, N. Mechanistic Studies on the Chiral Recognition of Polysaccharide-Based Chiral Stationary Phases Using Liquid Chromatography and Vibrational Circular Dichroism. *J. Chromatogr. A* **2009**, *1216*, 3784−3793.
(46) Wenslow; Wang, T. Solid-State NMR Characterization of Amylose Tris(3,5-Dimethylphenylcarbamate) Chiral Stationary-Phase Structure as a Function of Mobile-Phase Composition. *Anal. Chem.* **2001**, *73*, 4190−4195.
(47) Kasat, R. B.; Wang, N.-H. L.; Franses, E. I. Effects of Backbone and Side Chain on the Molecular Environments of Chiral Cavities in Polysaccharide-Based Biopolymers. *Biomacromolecules* **2007**, *8*, 1676−1685.
(48) Bereznitski, Y.; LoBrutto, R.; Variankaval, N.; Thompson, R.; Thompson, K.; Sajonz, P.; Crocker, L. S.; Kowal, J.; Cai, D.; Journet, M.; et al. Mechanistic Aspects of Chiral Discrimination on an Amylose Tris(3,5-Dimethylphenyl)Carbamate. *Enantiomer* **2002**, *7*, 305−315.
(49) Ye, Y. K.; Bai, S.; Vyas, S.; Wirth, M. J. NMR and Computational Studies of Chiral Discrimination by Amylose Tris-(3,5-Dimethylphenylcarbamate). *J. Phys. Chem. B* **2007**, *111*, 1189−1198.
(50) Li, Y.; Liu, D.; Wang, P.; Zhou, Z. Computational Study of Enantioseparation by Amylose Tris(3,5-Dimethylphenylcarbamate)-Based Chiral Stationary Phase. *J. Sep. Science* **2010**, *33*, 3245−3255.
(51) Tsui, H.-W.; Wang, N. H. L.; Franses, E. I. Chiral Recognition Mechanism of Acyloin-Containing Chiral Solutes by Amylose Tris[(S)-A-Methylbenzylcarbamate]. *J. Phys. Chem. B* **2013**, *117*, 9203−9216.
(52) Wang, T.; Wenslow, R. M., Jr. Effects of Alcohol Mobile-Phase Modifiers on the Structure and Chiral Selectivity of Amylose Tris(3,5-Dimethylphenylcarbamate) Chiral Stationary Phase. *J. Chromatogr. A* **2003**, *1015*, 99−110.
(53) Godschalk, F.; Genheden, S.; Soderhjelm, P. R.; Ryde, U. Comparison of MM/GBSA Calculations Based on Explicit and Implicit Solvent Simulations. *Phys. Chem. Chem. Phys.* **2013**, *15*, 7731−7739.
(54) Case, D. A.; Babin, V.; Berryman, J. T.; Betz, R. M.; Cai, Q.; Cerutti, D. S.; Cheatham, T. E., III; Darden, T. A.; Duke, R. E.; Gohlke, H.; Goetz, A. W.; Gusarov, S.; Homeyer, N.; Janowski, P.; Kaus, J.; Kolossváry, I.; Kovalenko, A.; Lee, T. S.; LeGrand, S.; Luchko, T.; Luo, R.; Madej, B.; Merz, K. M.; Paesani, F.; Roe, D. R.; Roitberg, A.; Sagui, C.; Salomon-Ferrer, R.; Seabra, G.; Simmerling, C. L.; Smith, W.; Swails, J.; Walker, R. C.; Wang, J.; Wolf, R. M.; Wu, X.; Kollman, P. A. *AMBER 14*; University of California: San Francisco, CA, 2014.
(55) Zhao, B.; Li, N. K.; Yingling, Y. G.; Hall, C. K. LCST Behavior Is Manifested in a Single Molecule: Elastin-Like Polypeptide $(VPGVG)_N$. *Biomacromolecules* **2016**, *17*, 111−118.
(56) Zhao, B.; Cohen Stuart, M. A.; Hall, C. K. Dock 'N Roll: Folding of a Silk-Inspired Polypeptide Into an Amyloid-Like Beta Solenoid. *Soft Matter* **2016**, *12*, 3721−3729.
(57) Berendsen, H. J. C.; Postma, J. P. M.; van Gunsteren, W. F.; DiNola, A.; Haak, J. R. Molecular Dynamics with Coupling to an External Bath. *J. Chem. Phys.* **1984**, *81*, 3684−3688.
(58) Essmann, U.; Perera, L.; Berkowitz, M. L.; Darden, T.; Lee, H.; Pedersen, L. G. A Smooth Particle Mesh Ewald Method. *J. Chem. Phys.* **1995**, *103*, 8577−8593.
(59) Ryckaert, J.-P.; Ciccotti, G.; Berendsen, H. J. C. Numerical Integration of the Cartesian Equations of Motion of a System with Constraints: Molecular Dynamics of N-Alkanes. *J. Comput. Phys.* **1977**, *23*, 327−341.
(60) Martínez, L.; Andrade, R.; Birgin, E. G.; Martínez, J. M. PACKMOL: a Package for Building Initial Configurations for Molecular Dynamics Simulations. *J. Comput. Chem.* **2009**, *30*, 2157−2164.
(61) Shenkin, P. S.; Mcdonald, D. Q. Cluster Analysis of Molecular Conformations. *J. Comput. Chem.* **1994**, *15*, 899−916.
(62) Kleywegt, G. J.; Jones, T. A. Phi/Psi-Chology: Ramachandran Revisited. *Structure* **1996**, *4*, 1395−1400.

DOI: 10.1021/acs.langmuir.7b02337
Langmuir 2017, 33, 11246−11256